ACS APPLIED MATERIALS & INTERFACES

Letter

www.acsami.org

# Improved Thermal Oxidation Stability of Solution-Processable Silver Nanowire Transparent Electrode by Reduced Graphene Oxide

Yumi Ahn, Youngjun Jeong, and Youngu Lee*

Department of Energy Systems Engineering, Daegu Gyeongbuk Institute of Science and Technology (DGIST), 50-1 Sang-Ri, Hyeonpung-Myeon, Dalseong-Gun, Daegu, 711-873, Korea

Supporting Information

**ABSTRACT:** Solution-processable silver nanowire-reduced graphene oxide (AgNW-rGO) hybrid transparent electrode was prepared in order to replace conventional ITO transparent electrode. AgNW-rGO hybrid transparent electrode exhibited high optical transmittance and low sheet resistance, which is comparable to ITO transparent electrode. In addition, it was found that AgNW-rGO hybrid transparent electrode exhibited highly enhanced thermal oxidation and chemical stabilities due to excellent gas-barrier property of rGO passivation layer onto AgNW film. Furthermore, the organic solar cells with AgNW-rGO hybrid transparent electrode showed good photovoltaic behavior as much as solar cells with AgNW transparent electrode. It is expected that AgNW-rGO hybrid transparent electrode can be used as a key component in various optoelectronic application such as display panels, touch screen panels, and solar cells.

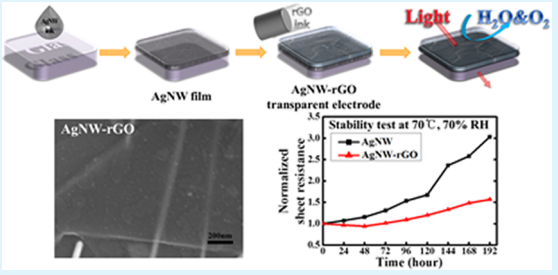


**KEYWORDS:** *silver nanowire, reduced graphene oxide, transparent electrode, thermal oxidation stability, organic solar cell*

## INTRODUCTION

Transparent and conducting metal oxides such as indium tin oxide (ITO) have been widely used as an essential element of various optoelectronic devices such as liquid crystal display (LCD) panels, organic light-emitting diode(OLED) panels, touch screen panels, e-paper, and solar cells.[1−4] Vacuum-deposited ITO transparent electrode possesses good physical properties such as high optical transmittance and low sheet resistance as a transparent electrode for various optoelectronic devices.[5] However, it has several drawbacks such as brittleness, color, low optical transmittance in near-infrared (NIR), and high processing temperature.[6] Furthermore, the scarcity of indium resources makes ITO transparent electrode very expensive recently. Therefore, cheap, flexible, and solution-processable transparent electrodes have been required for next generation of optoelectronic devices such as flexible solar cells and displays.[7−9] Recently, new transparent electrode materials such as graphene, carbon nanotubes (CNT), conductive polymer, metal grid, and Ag nanowire(AgNW) films have been developed to replace conventional ITO transparent electrode.[10−16]

Among various ITO alternatives, AgNW films already showed the good optical and electrical performance comparable to ITO.[17,18] AgNW films can be fabricated by solution processes such as spin, slot die, or bar coatings. In addition, AgNW films on plastic substrates already exhibited good flexibility and mechanical stability. However, they still have a long-term stability issue, which makes them difficult for practical use.[19] When AgNW films are exposed to air and water, AgNW can be easily oxidized, leading to sharp increase of sheet resistance and hazeness of the AgNW films.[20] Therefore, it is necessary to suppress the oxidation of AgNWs for enhancement of the long-term stability of the AgNW films.

In this manuscript, we demonstrate reduced graphene oxide (rGO)-coated AgNW films which exhibit excellent thermal oxidation and chemical stabilities. Graphene has been widely studied for its remarkable electrical and mechanical properties. Furthermore, it is well-known that graphene is impermeable to all gases. More recently, graphene has been used as a passivation layer with excellent performance by preventing the oxidation of metals such as copper and nickel.[21] Therefore, we introduce rGO onto pristine AgNW films to protect AgNWs from ambient condition without loss of electrical and optical properties of the AgNW films. The reduced graphene oxide (rGO)-coated AgNW films exhibited high optical transmittance and low sheet resistance, which is comparable to ITO transparent electrode. In addition, it was found that AgNW-rGO films exhibited highly enhanced long-term stability due to excellent gas-barrier property of rGO passivation layer onto AgNW film.

## RESULTS AND DISCUSSION

AgNW films were prepared by spin-coating AgNW inks on glass substrates. To prepare AgNW films on glass substrates, we treated glass substrates with UV/Ozone to make hydrophilic surfaces for AgNW spin-coating. Then, AgNW ink was spin-coated on a glass substrate and then dried at 120°C for 5 min. Several AgNW films were prepared by changing spin-coating speed from 250 to 2000 rpm to investigate the effect of spin-

Received: September 6, 2012
Accepted: December 3, 2012
Published: December 3, 2012

  

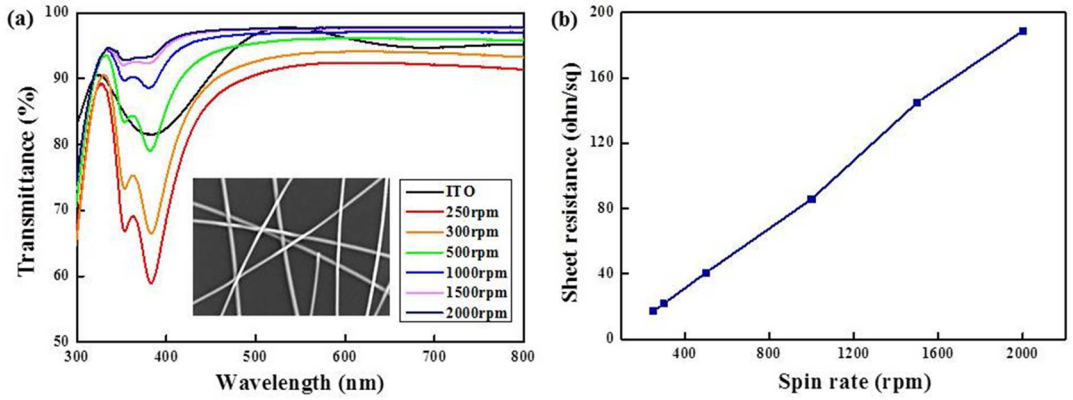


**Figure 1.** (a) Optical transmittance spectra for AgNW films on glass substrates, which are coated with different spin-coating speeds and conventional ITO transparent electrode with the sheet resistance of 12 Ω/sq. The inset is a SEM image of AgNW film. AgNWs, which have 40 nm diameter and >20 $\mu$m length are coated on glass by spin coating at 2000 rpm. (b) Sheet resistance of AgNW films as a function of spin-coating rates.

coating speed on optical and electrical properties of AgNW films. Figure 1 shows optical transmittance spectra and sheet resistance of AgNW films on glass substrates between 250 rpm and 2000 rpm in spin-coating speed.

As shown in Figure 1a inset, average length and diameter of AgNWs are about 10 $\mu$m and 40 nm, respectively. A random network of AgNWs provides electron transporting channels, leading to low sheet resistance of the resulting AgNW films. In addition, hollow spaces inside the AgNW network and diffusive reflection from AgNWs result in high optical transmittance. As shown in Figure 1, when the spin-coating speed increased from 250 to 2000 rpm, optical transmittance and sheet resistance were increased from 92.0 to 97.7% at 550 nm and from 17.3 to 204.5 Ω/sq, respectively, indicating that optical transmittance and sheet resistance of AgNW films increased as the spin-coating speed increased. This result confirms that the increased spin-coating speeds can lead to higher transparency and lower conductivity by reducing the density of AgNWs on the substrate.

It was found that AgNW films showed relatively high optical transmittance in visible wavelength region compared to ITO. In addition, the optical transmittance of the AgNW films is constant in the near-infrared (NIR) regions, indicating that high transmittance in broad range of wavelength allows the AgNW films to be used for a variety of optoelectronic devices.[14,22]

One of the drawbacks of AgNW films is that AgNW can be easily oxidized when it is exposed to ambient condition for a long time. Therefore, thermal oxidation stability of the AgNW films is much poorer than the competing transparent conductors such as CNT and graphene.

To enhance thermal oxidation stability of AgNW based transparent electrode, we fabricated AgNW−reduced graphene (rGO) hybrid transparent electrode by solution process. It is well-known that graphene is impermeable to gas molecules. The capability of graphene coating has been proved as the protection layer by exposing a graphene-coated metal to liquid etchant and annealing.[21]

AgNW−graphene hybrid transparent electrode was prepared by coating reduced graphene oxide (rGO) onto the AgNW film. Firstly, rGO was synthesized by reducing graphene oxide in the presence of iodine.[23−25] Then, rGO solution was prepared by dispersing 1 mg of graphene in 20 mL of deionized water. The rGO solution was ultrasonicated for 1 day for complete dispersion. To coat rGO onto the AgNW film, we dipped the AgNW film in the rGO solution for 30 s and then dried for 5 min at 120 °C. By repeating this process, multilayers of rGO could be coated onto the AgNW film successfully. Figure 2 shows the

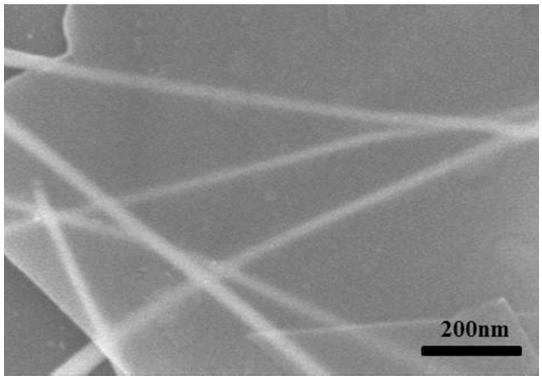


**Figure 2.** SEM image of reduced graphene oxide (rGO)-coated AgNW film.

SEM image of the AgNW−rGO hybrid transparent electrode by sequential coating of rGO on the AgNW film, confirming that the AgNW film was covered with rGO by dip-coating process.

To investigate optical and electrical properties of the AgNW−rGO hybrid transparent electrode, the optical transmittance and sheet resistance of the AgNW-rGO films were measured as a function of the number of dip-coating of rGO solution.

As shown in Figure 3a, the optical transmittance of the AgNW−rGO film decreased as the number of rGO dip-coating increased, suggesting that rGO was successfully coated onto the AgNW film. After five times of rGO dip-coating onto AgNW film, the optical transmittance of the resulting AgNW−rGO film showed about 2% decrease at 550 nm. However, it was found that the optical transmittance of the AgNW−rGO film increased in the wavelength ranging from 350 to 450 nm compared to AgNW film. It is generally expected that the optical transmittance of AgNW−rGO film should be lower than the pristine AgNW film because rGO could absorb additional photons throughout the entire wavelength range. This unexpected phenomenon can be explained by decreased plasmon absorption of AgNW−rGO. In noble metals, the decrease in size below the electron mean free path induces intense plasmon absorption in short wavelength.[26] Therefore, as for AgNW films, decreased optical transmittance can be obtained around 400 nm due to plasmon absorption of AgNWs.[27] However, AgNW−rGO films showed enhanced


dx.doi.org/10.1021/am301913w | ACS Appl. Mater. Interfaces 2012, 4, 6410−6414

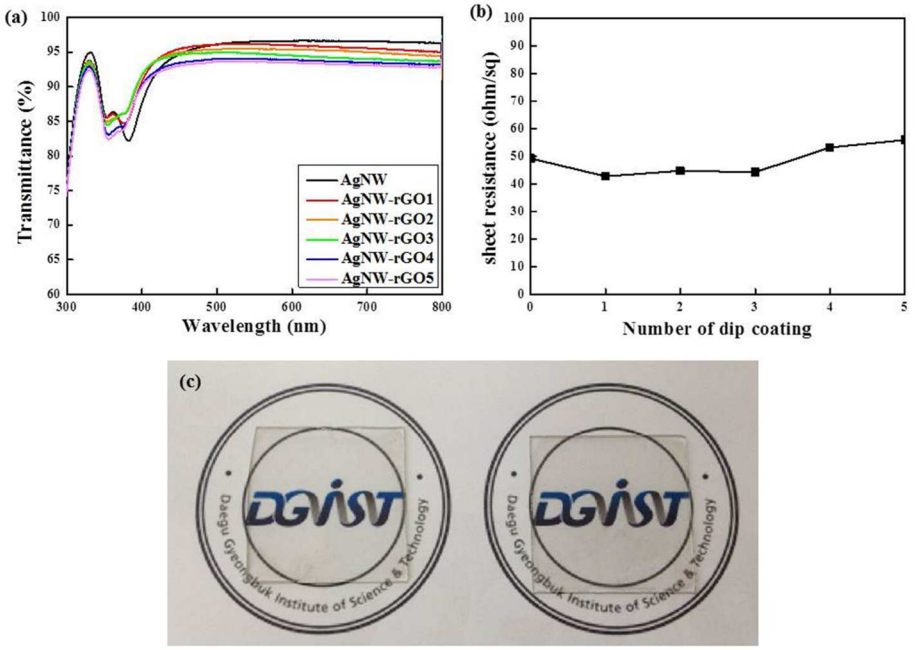


**Figure 3.** (a) Optical transmittance spectra for AgNW−rGO film with different dip-coating number in rGO solution. (b) Sheet resistance of AgNW−rGO films with different dip-coating numbers in rGO solution. (c) Images of AgNW film (left) and AgNW−rGO (right) films on glass substrates.

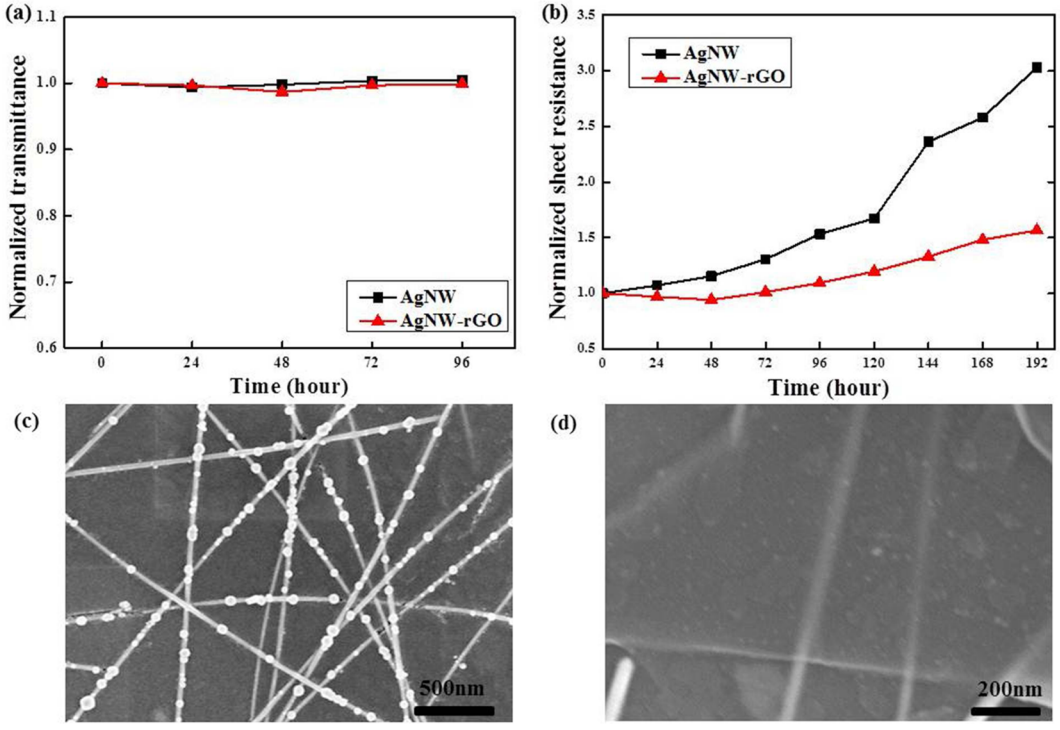


**Figure 4.** Stability tests of AgNW and AgNW−rGO films at 70 °C and 70% RH. (a) Optical transmittance as a function of time for 4 days. (b) Sheet resistance change as a function of exposing time. SEM images of (c) AgNW film and (d) AgNW−rGO film after the stability test (70 °C and 70% RH for 8 days).

optical transmittance from 350 nm to 450 nm. The increased optical transmittance around 400 nm might be caused by reduced plasmon absorption because the conductive rGO, which partially covers the long and thin AgNWs, decreases the collective oscillation of the free electrons through AgNWs induced by an interacting electromagnetic field.[28−32]

Figure 3b shows the relationship between the sheet resistance of AgNW−rGO films and the number of rGO dip-coating. It was found that the sheet resistance of AgNW−rGO films was not affected by the number of rGO coating. This result indicates that the total sheet resistance of AgNW−rGO film could be determined by the AgNW film because AgNW is much more conductive than rGO.[33]


dx.doi.org/10.1021/am301913w | ACS Appl. Mater. Interfaces 2012, 4, 6410−6414

Flexible AgNW−rGO film was prepared onto a polyethylene naphthalate (PEN) substrate for assessment of flexibility. Then, the bending test of AgNW−rGO PEN film was performed by varying the bending radius of the films. The change of sheet resistance of AgNW−rGO film was measured while it was bent from 20 to 8 mm in radius of curvature (see Figure-S1 in the Supporting Information). Even though AgNW−rGO film was bent to radius of 8 mm, the sheet resistance of the film was not changed. The sheet resistance of ITO film, on the other hand, started to increase at radius of 16 mm and increased over 100 times at radius of 8 mm. It was found that the dramatic increase in sheet resistance of ITO was attributed to the formation of micro cracks, as shown in Figure-S2 in the Supporting Information.[34] This result clearly shows that highly flexible transparent electrode can be fabricated by coating AgNW−rGO on plastic substrates.

To evaluate the effect of rGO layer on thermal oxidation stability of AgNW-rGO film, we exposed AgNW and AgNW-rGO films at high temperature (70 °C) and high humidity (70% RH) condition for 8 days. Figure 4 shows the changes in optical transmittance and sheet resistance of the films for thermal oxidation stability test. The optical transmittance of both samples has no significant change (Figure 4a). However, as shown in Figure 4b, the sheet resistance of AgNW film increased more than 300% when it was exposed at 70 °C and 70% RH for 8 days. It has been well-known that AgNW is easily oxidized when it is exposed to air.[18] When AgNWs are oxidized, the single NW and the junction resistance would increase because of the formation of silver oxide on the surface of AgNW.[19] In contrast, the sheet resistance of AgNW−rGO film was slightly increased less than 50%, even at 70 °C and 70% RH for 8 days. This huge difference in change of sheet resistance between AgNW and AgNW−rGO films confirms that AgNW−rGO film possesses high thermal oxidation stability compared to AgNW film because additional rGO layer is impermeable to oxygen molecules. Moreover, it was found that the sheet resistance of AgNW−rGO film was slightly decreased in the initial 48 h. This result might be due to the enhanced conductivity of rGO during thermal treatment.[35]

SEM images of AgNW and AgNW−rGO films after stability test were measured in order to investigate the cause for the enhanced thermal oxidation stability in AgNW−rGO film (Figure 4c, d). X-ray diffraction (XRD) and energy dispersive spectroscopy (EDS) measurements of AgNW film clearly confirms the formation of silver oxides onto AgNW after the thermal oxidation stability test (see Figure-S3 in the Supporting Information). In the case of AgNW film, it was found that silver oxides were formed on silver nanowire surface, indicating that these oxides are the major cause of increased sheet resistance.[19] In contrast, AgNW−rGO film did not have silver oxides because gas and moisture cannot permeate the rGO layer because of the good property as gas and moisture barriers.[36] It means that these gas barrier properties of graphene prevent the oxidation of AgNW with exclusion of air and moisture. Therefore, AgNW−rGO film showed little change of sheet resistance rather than AgNW film. These results clearly indicate that the graphene coating protects the underlying AgNW from oxidation, and then long-term stability of AgNW films improves. Therefore, it is expected that the sheet resistance in AgNW−rGO film will be maintained constantly if the whole surface of the AgNW film is completely covered with graphene.

To test the performance of AgNW−rGO film as the transparent electrode, we used AgNW and AgNW−rGO films as anode layers in bulk heterojunction polymer solar cells. Firstly, AgNW pattern for the anode layer was prepared onto a glass substrate by spin coating and photolithography process. As for AgNW−rGO transparent electrode, patterned AgNW film was dipped into the aqueous solution of rGO. The bulk heterojunction solar cells were then fabricated on AgNW and AgNW−rGO transparent electrodes with a 30 nm of poly(3,4-ethylenedioxythiophene):poly(styrenesulfonate) (PEDOT:PSS), 100 nm of a P3HT and PCBM blend with a 1:1 ratio, and LiF/Al cathode. It was found that some AgNWs without rGO layer were etched out due to acidic PEDOT:PSS layer (see Figure S4 in the Supporting Information).[37,38] However, the rGO-covered AgNW layers showed resistance against corrosion even though the PEDOT:PSS solution was coated onto the AgNW, confirming that the rGO layer provides chemical inertness against acidic condition for AgNWs. Thus, the enhanced chemical stability of AgNW−rGO film against acidic condition may affect the power conversion efficiency (PCE) of the solar cell devices.

Figure 5 shows the current density−voltage ($J$−$V$) characteristics of bulk heterojunction polymer solar cells with AgNW and AgNW−rGO transparent electrodes under illumination. In the case of solar cells with AgNW−rGO transparent electrode, it showed an open-circuit voltage ($V_{oc}$) of 0.49, short- circuit current density ($J_{sc}$) of 6.38 mAcm$^{-2}$, and fill factor (FF) of 32.91, resulting in power conversion efficiency (PCE) of 1.03%. In control devices with the AgNW transparent electrode, the PCE is 1.20% with a $V_{oc}$ of 0.49 V, a $J_{sc}$ of 6.42 mA cm$^{-2}$, and a FF of 38.25. This result clearly indicates that the solar cells with AgNW−rGO transparent electrode perform as much as that with AgNW transparent electrode. Compared to the control devices, the solar cells with AgNW−rGO transparent electrode exhibited a little lower $J_{sc}$ because of the decreased optical transmittance. It is found that the FF of the solar cells with AgNW−rGO transparent electrode is lower than that of AgNW-based solar cells. This result might be caused by increased roughness of AgNW−rGO transparent electrode. If rGO layer is uniformly coated onto AgNW transparent electrode, the PCE of the solar cells may be improved.

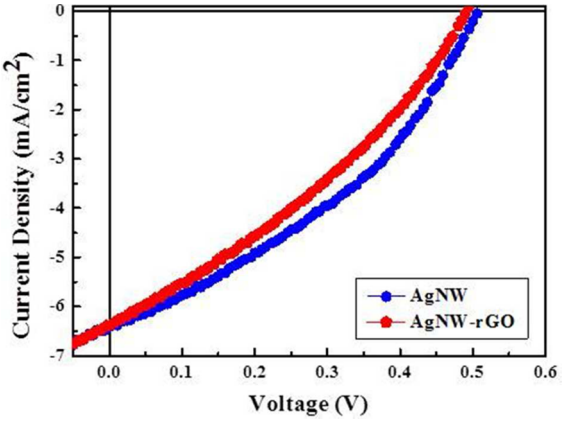


**Figure 5.** Current density−voltage ($J$−$V$) characteristics of bulk heterojunction polymer solar cells with AgNW and AgNW-rGO transparent electrodes.

## CONCLUSION

Solution-processable AgNW−rGO hybrid transparent electrode was prepared in order to replace conventional ITO transparent electrode. AgNW−rGO hybrid transparent electrode exhibited high optical transmittance and low sheet resistance, which is

comparable to ITO transparent electrode. AgNW−rGO film showed good flexibility when it was fabricated on plastic substrates. It was also found that AgNW−rGO films exhibited highly enhanced thermal oxidation and chemical stabilities because of the excellent gas-barrier property of rGO passivation layer onto AgNW film. Furthermore, the solar cells with AgNW−rGO transparent electrode showed good photovoltaic behavior. We anticipate that AgNW−rGO transparent electrode can be used as an alternative of ITO transparent electrode for various optoelectronic devices such as solar cells, OLEDs, and touch panels.

## ■ ASSOCIATED CONTENT

### Supporting Information

Detailed fabrication processes of AgNW and AgNW-rGO films, and organic photovoltaic devices. This material is available free of charge via the Internet at http://pubs.acs.org

## ■ AUTHOR INFORMATION

### Corresponding Author

*E-mail: youngulee@dgist.ac.kr.

### Notes

The authors declare no competing financial interest.

## ■ ACKNOWLEDGMENTS

This work was supported by the DGIST R&D Program of the Ministry of Education, Science, and Technology of Korea (12-BD-0405). This research was also supported by Basic Science Research Program through the National Research Foundation of Korea (NRF) funded by the Ministry of Education, Science, and Technology (2012R1A1A1040811). We gratefully acknowledge Cambrios Technologies Corporation for AgNW ink.

## ■ REFERENCES

(1) Chen, S.; Deng, L.; Xie, J.; Peng, L.; Xie, L.; Fan, Q.; Huang, W. *Adv. Mater.* **2010**, *22*, 5227−5239.
(2) Layani, M.; Gruchko, M.; Milo, O.; Balberg, I.; Azulay, D.; Magdassi, S. *ACS Nano* **2009**, *3*, 3537−3542.
(3) Sun, Y.; Welch, G. C.; Leong, W. L.; Takacs, C. J.; Bazan, G. C.; Heeger, A. J. *Nat. Mater.* **2012**, *11*, 44−48.
(4) Granqvist, C. G. *Sol. Energy Mater. Sol. Cells* **2007**, *91*, 1529−1598.
(5) Han, H.; Adams, D.; Mayer, J. W.; Alford, T. L. *J. Appl. Phys.* **2005**, *98*, 083705.
(6) Hecht, D. S.; Hu, L.; Irvin, G. *Adv. Mater.* **2011**, *23*, 1482−1513.
(7) De, S.; Higgins, T. M.; Lyons, P. E.; Doherty, E. M.; Nirmalraj, P. N.; Blau, W. J.; Boland, J. J.; Coleman, J. N. *ACS Nano* **2009**, *3*, 1767−1774.
(8) Krebs, F. C.; Gevorgyan, S. A.; Alstrup, J. *J. Mater. Chem.* **2009**, *19*, 5442−5451.
(9) Krebs, F. C. *Org. Electron.* **2009**, *10*, 761−768.
(10) Liu, Z. K.; Li, J. H.; Sun, Z. H.; Tai, G. A.; Lau, S. P.; Yan, F. *ACS Nano* **2012**, *6*, 810−818.
(11) Kim, K. S.; Zhao, Y.; Jang, H.; Lee, S. Y.; Kim, J. M.; Kim, K. S.; Ahn, J. H.; Kim, P.; Choi, J. Y.; Hong, B. H. *Nature* **2009**, *457*, 706−710.
(12) Wang, X.; Zhi, L.; Müllen, K. *Nano Lett.* **2008**, *8*, 323−327.
(13) Wu, Z. C.; Chen, Z. H.; Du, X.; Logan, J. M.; Sippel, J.; Nikolou, M.; Kamaras, K.; Reynolds, J. R.; Tanner, D. B.; Hebard, A. F.; Rinzler, A. G. *Science* **2004**, *305*, 1273−1276.
(14) Na, S. I.; Kim, S. S.; Jo, J.; Kim, D. Y. *Adv. Mater.* **2008**, *20*, 4061−4067.
(15) Lee, J. Y.; Connor, S. T.; Cui, Y.; Peumans, P. *Nano Lett.* **2008**, *8*, 689−692.
(16) Leem, D. S.; Edwards, A.; Faist, M.; Nelson, J.; Bradley, D. D. C.; de Mello, J. C. *Adv. Mater.* **2011**, *23*, 4371−4375.
(17) Yu, Z.; Zhang, Q.; Li, L.; Chen, Q.; Niu, X.; Liu, J.; Pei, Q. *Adv. Mater.* **2011**, *23*, 664−668.
(18) Krantz, J.; Richter, M.; Spallek, S.; Spiecker, E.; Brabec, C. J. *Adv. Funct. Mater.* **2011**, *21*, 4784−4787.
(19) Elechiguerra, J. L.; Larios-Lopez, L.; Liu, C.; Garcia-Gutierrez, D.; Camacho-Bragado, A.; Yacaman, M. J. *Chem. Mater.* **2005**, *17*, 6042−6052.
(20) Liu, C. H.; Yu, X. *Nanoscale Res. Lett.* **2011**, *6*, 75.
(21) Chen, S.; Brown, L.; Levendorf, M.; Cai, W.; Ju, S. Y.; Edgeworth, J.; Li, X.; Magnuson, C. W.; Velamakanni, A.; Piner, R. D.; Kang, J.; Park, J.; Ruoff, R. S. *ACS Nano* **2011**, *5*, 1321−1327.
(22) Hu, L.; Kim, H. S.; Lee, J. Y; Peumans, P.; Cui, Y. *ACS Nano* **2010**, *4*, 2955−2963.
(23) Hummers, W. S.; Offeman, R. E. *J. Am. Chem. Soc.* **1958**, *80*, 1339.
(24) Cote, L. J.; Kim, F.; Huang, J. *J. Am. Chem. Soc.* **2009**, *131*, 1043−1049.
(25) Moon, I. K.; Lee, J.; Ruoff, R. S.; Lee, H. *Nat. Commun.* **2010**, *1*, 1−6.
(26) El-Sayed, M. A. *Acc. Chem. Res.* **2001**, *34*, 257−264.
(27) Graff, A.; Wagner, D.; Ditlbacher, H.; Kreibig, U. *Eur. Phys. J. D* **2005**, *34*, 263−269.
(28) Martin, Y. C.; Hamann, H. F.; Wickramasinghe, H. K. *J. Appl. Phys.* **2001**, *89*, 5774.
(29) Sun, Y.; Gates, B.; Mayers, B.; Xia, Y. *Nano Lett.* **2002**, *2*, 165−168.
(30) Zhang, D.; Qi, L.; Yang, J.; Ma, J.; Cheng, H.; Huang, L. *Chem. Mater.* **2004**, *16*, 872−876.
(31) Yang, L.; Li, G. H.; Zhang, L. D. *Appl. Phy. Lett.* **2000**, *76*, 1537−1539.
(32) Link, S.; El-Sayed, M. A. *J. Phys. Chem. B* **1999**, *103*, 4214−4217.
(33) Kumar, A.; Zhou, C. *ACS Nano* **2010**, *4*, 11−14.
(34) Cairns, D. R.; Witter, R. P.; Sparacin, D. K.; Sachsman, S. M.; Paine, D. C.; Crawford, G. P.; Newton, R.R. *Appl. Phys. Lett.* **2000**, *76*, 1425−1427.
(35) Chang, H.; Sun, Z.; Yuan, Q.; Ding, F.; Tao, X.; Yan, F.; Zheng, Z. *Adv. Mater.* **2010**, *22*, 4872−4876.
(36) Kim, H.; Miura, Y.; Macosko, C. W. *Chem. Mater.* **2010**, *22*, 3441−3450.
(37) Yang, L.; Zhang, T.; Zhou, H.; Price, S. C.; Wiley, B. J.; You, W. *ACS Appl. Mater. Interfaces* **2011**, *3*, 4075−4084.
(38) Hsu, P. C.; Wu, H.; Carney, T. J.; McDowell, M. T.; Yang, Y.; Garnett, E. C.; Li, M.; Hu, L.; Cui, Y. *ACS Nano* **2012**, *6*, 5150−5156.